ACADEMIA ROMÂNĂ
*Revue Roumaine de Chimie*
http://web.icf.ro/rrch/

*Rev. Roum. Chim.*,
**2019**, *64*(8), 711-717
DOI: 10.3224/rrch.2019.64.8.07

# PREPARATION AND ENHANCED ELECTROCATALYTIC PERFORMANCES OF $Co_3O_4$ COMPOSITES NANOSHEETS LOADED WITH DOUBLE PRECIOUS METALS

Lu PAN[a,b,*]

[a] School of Chemistry and Materials Engineering, Huainan Normal University, Huainan 232038, Anhui, People's Republic of China
[b] Anhui Key Laboratory of Low temperature Co-fired Material, Huainan Normal University, Huainan 232001, China

*Received November 26, 2018*

A facile and easily controlled one-step procedure was designed to prepare the precursors of $Co_3O_4$, $Au/Co_3O_4$ and $Ag_xAu_y/Co_3O_4$ with 2% Au and different Ag contents at 140 °C for 15 h. The resultant $Co_3O_4$, $Au/Co_3O_4$ and $Ag_xAu_y/Co_3O_4$ composite nanosheets could be fabricated by incinerating their precursors at 400 °C for 3 h. The as-prepared samples presented sheet-like morphology. Both Au and Ag nanoparticles with the mean sizes less than 10 nm were dispersed finely on $Co_3O_4$ nanosheets. The electrocatalytic performances of final samples modified on the glassy carbon electrode for *p*-nitrophenol reduction in a basic solution were investigated. The results demonstrated doping of Ag and Au nanoparticles could effectively enhance the electrocatalytic activity.

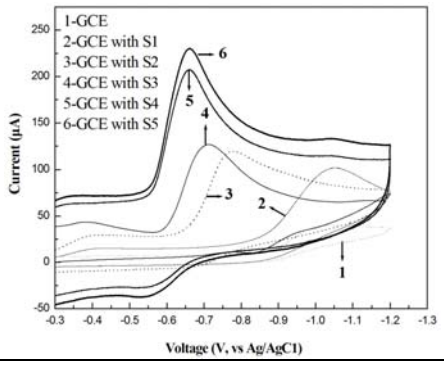


## INTRODUCTION

$Co_3O_4$ is an important transition metal oxide with a cubic spinel structure. In the past decades, $Co_3O_4$ nanomaterials with different morphologies have been synthesized via numerous methods.[1-3] To further expand the application of $Co_3O_4$ nanomaterials, the synthesis and properties of $Co_3O_4$ composites have attracted extensive attentions. Frequently, the $Co_3O_4$ composites can exhibit more novel, significant or enhanced properties than the pure $Co_3O_4$ nanomaterials.

Although the $Co_3O_4$ composites have been studied extensively, their properties mainly focus on the catalysis. For the inorganic composites of $Co_3O_4$, the synthesis and catalytic properties of noble metals/$Co_3O_4$ composites have been investigated widely.[4-6] As well known, the noble metals can exhibit excellent catalytic performances in many fields.[7-10] Among the noble metals, silver has been used in a high frequency because of its low price and stable properties. So Ag nanoparticles are loaded frequently on the transition metal oxides to form the composite nanomaterials. Ag/$Co_3O_4$ composite nanostructures have been studied overwhelmingly in catalytic fields, which are not found in the individual component but can expand their performances.[11–14]

To further raise the catalytic properties of $Co_3O_4$ composites doped with single noble metal, much effort has been made to design the double noble metals/$Co_3O_4$ composites. Loading with double noble metals may achieve the synergetic catalysis effect between two noble metals. The synthesis of double noble metals/$Co_3O_4$ composites is full of huge challenge. Generally, multiple steps

* Corresponding author: panlu2008@163.com; Fax: +86554 6672650

are used to prepare the double noble metals/$Co_3O_4$ composites.[12] $Co_3O_4$ nanomaterial synthesized first then the noble metals are loaded seriatim. The preparation procedures are complicated. In the work, we had designed a facile and easily controlled one-step procedure to prepare the precursors of $Ag_xAu_y/Co_3O_4$ composite nanosheets, and the final samples could be fabricated by calcining the precursors at 400 °C for 3 h. The as-synthesized samples were modified on a glassy carbon electrode and their electrocatalytic performances for *p*-nitrophenol reduction had been examined, and their excellent catalytic property suggests the potential application in electrocatalysis sphere.

## EXPERIMENTAL

### 1. Chemicals

$AgNO_3$, $HAuC1_4$, $Co(NO_3)_2{\cdot}6H_2O$, $Na_2CO_3$ and potassium sorbate were purchased from Shanghai Chemical Reagent Co., China. All reagents were of analytical grade and used as received without further purification.

### 2. Preparation of $Ag_xAu_y/Co_3O_4$ composite samples

The desired $Ag_xAu_y/Co_3O_4$ composite nanomaterials were synthesized by using an easily controlled hydrothermal procedure. For each synthesis, the total amount of $Co(NO_3)_2{\cdot}H_2O$, $HAuC1_4$ and $AgNO_3$ was fixed at 10.0 mmol. Typically, a certain amount of $Co(NO_3)_2{\cdot}6H_2O$, the demanded amount of $AgNO_3$ and 0.20 mmol of $HAuC1_4$ (for preparation $Co_3O_4$, no $HAuC1_4$ was added) were added to a beaker containing 60 mL of distilled water. These solutes were dissolved completely under stirring. Subsequently, 5.0 g of potassium sorbate was added directly to the beaker and was dissolved under stirring. Immediately, a large quantity of precipitate appeared. The stirring was kept for 20 min. The 60 mL of solution containing 10 mmol of $Na_2CO_3$ was added to the beaker by dropwise with the continuous stirring. After addition of $Na_2CO_3$ solution, the stirring was kept for 20 min. Finally, the mixture was transferred into 150 mL of Teflon-lined stainless steel autoclave and maintained in an electrically heated drying oven at 140 °C for 15 h. As the autoclave was cooled to room temperature naturally, and the precipitate was filtered and washed with distilled water then ethanol for several times, and dried in vacuum at 80 °C for 6 h. With altering the addition of $AgNO_3$, a series of precursors were prepared. By calcining the dried precursors at 400 °C according to the TG test experimental, the $Co_3O_4$, (S1), $Au/Co_3O_4$ with 2% Au (S2), $Ag_xAu_y/Co_3O_4$ with 1% Ag and 2% Au (S3), $Ag_xAu_y/Co_3O_4$ with 2% Ag and 2% Au (S4) and $Ag_xAu_y/Co_3O_4$ with 3% Ag and 2% Au (S5), were prepared, respectively. As a comparison, $Co_3O_4$ nanoparticles had been prepared without addition potassium sorbate.

The detailed compositions and final samples are listed in Table 1.

### 3. Characterization of the samples

The thermogravimetric analysis of the precursor was carried out on a Shimadzu TA-50WS analyzer in $N_2$ gas in the temperature range from room temperature to 850 °C. The XRD parrerns of the as-synthesized samples was examined on a Philips X'Pert PROSUPER X-ray diffraction (XRD) with Cu Kα radiation (λ=0.154178 nm), using an operation voltage and current of 40 kV and 50 mA. The TEM images were collected on a Hitachi Model H-800 transmission electron microscopy, using an accelerating voltage of 200kV. XPS was performed using an ESCALAB 250 VG Lited XPS operated at 15 kV (hν = 1486.6 eV).

### 4. Electrocatalytic activity examination

The electrocatalytic performances of the as-synthesized samples modified on a glassy carbon electrode (GCE) for the reduction of *p*-nitrophenol in a basic solution were performed on LK 98 microcomputer-based electrochemical system (Tianjin Lanlike Chemical and Electron High Technology Co., Ltd., Tianjin in China). During the testing, a three-electrode single compartment cell was used for cyclic voltammetry determination. A GCE (3.7 mm diameter) and a platinum plate served as the working and counter electrode, respectively, and a Ag/AgC1 electrode was used as the reference electrode. Before each measurement, the GCE surface was carefully polished on an abrasive paper first, then further polished with 0.3 and 0.05 μm α-$Al_2O_3$ paste in turn, finally rinsed thoroughly with doubly distilled water and absolute alcohol. A 20 mg of sample was dispersed in 4 mL of doubly distilled water under ultrasonication to form a suspension solution. Of the suspension one, 50 μL was taken out and covered on the carbon surface of the GCE in a good reversible state. After being dried spontaneously in air, the modified GCE was prepared and used directly for electrochemical determination.

## RESULTS AND DISCUSSION

### 1. The TG test of $Co_3O_4$ precursor

To get the suitable incineration temperature of the precursors transferring into the final samples, the $Co_3O_4$ precursor was chosen to carry out the TG experiment. The result is displayed in Fig. 1. Based on Fig. 1, by heating the precursor in the range from room temperature to 850 °C, only one weight loss plat locating at the interval of 250-320 °C can be seen clearly, and the weight loss value is about 23%. In the weight loss interval, the precursor is incinerated and transferred into the final sample. With increasing the temperature from room temperature to 250 °C, a weight loss with 3% value due to desorption of smaller molecules absorbed on the precursor. If increasing the temperature from 320 to 850 °C, no weigh loss occurs, indicating the stable existence of the final $Co_3O_4$ at the temperature more than 320 °C. In the work, the $Co_3O_4$ sample was fabricated by incinerating its precursor at 400 °C for 3 h. For the precursor containing Ag or Au, Ag(I) or Au(III) ions might be reduced by sorbate anions. As well known, Ag or Au metal is stable as the temperature is more than 400 °C. In a whole, $Co_3O_4$, $Au/Co_3O_4$ and $Ag_xAu_y/Co_3O_4$ composites can be prepared by calcining the corresponding precursors at 400 °C for 3 h.

*Table 1*

The raw metal compound compositions for synthesis of the samples

| Sample | S1 | S2 | S3 | S4 | S5 |
|---|---|---|---|---|---|
| $Co(NO_3)_2$ (mmol) | 10.0 | 9.8 | 9.7 | 9.6 | 9.5 |
| $AgNO_3$ (mmol) | 0 | 0 | 0.1 | 0.2 | 0.3 |
| $HAuC1_4$ (mmol) | 0 | 0.2 | 0.2 | 0.2 | 0.2 |

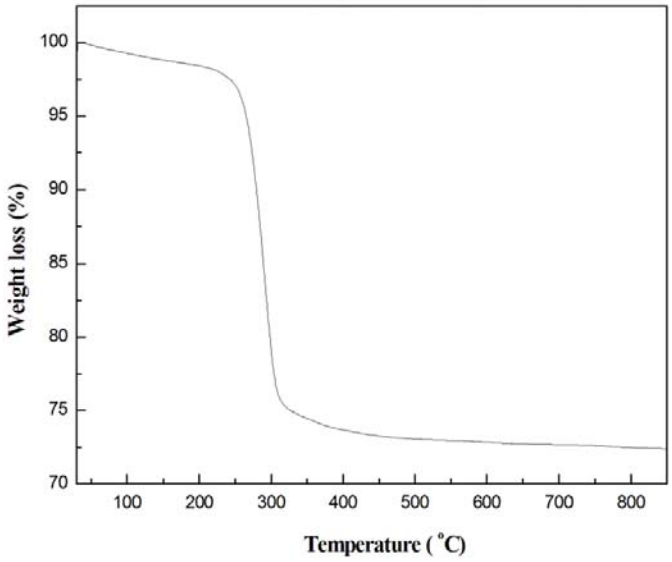


Fig. 1 – TG curve of $Co_3O_4$ precursor.

## 2. The phases and morphologies of the final samples

To investigate the phases and compositions, the XRD patterns of $Co_3O_4$ (S1), $Au/Co_3O_4$ with 2% Au (S2) and $Ag_xAu_y/Co_3O_4$ composite with 2% Ag and 2% Au (S4) were detected. The results are shown in Fig. 2. The curve of S1 demonstrates that all diffraction peaks are in good agreement with cubic $Co_3O_4$ phase with a spinel structure, no impure peaks belonging to CoOOH, CoO and $Co_2O_3$ phases can be detected, confirming the formation of pure $Co_3O_4$. From the curve of S2, except for the characteristic diffraction peaks of $Co_3O_4$, other two diffraction peaks locating at 38 and 44 $^o$ in 2θ which are attributed to the (111) and (200) crystal planes of the face-centered cubic Au have been discovered clearly. It is known, another (220) plane ascribed to the cubic Au metal might stand at 64$^o$ in 2θ. By comparison with curve of S1 and S2, the diffraction peak of (440) plane of cubic $Co_3O_4$ locating at 65$^o$ broadens markedly, furthermore, the diffraction intensity of (220) plane of Au at 64$^o$ is rather weak, so the diffraction peak of (220) plane of Au at 64$^o$ may be overlapped. As for the curve of S4, the characteristic diffraction peaks are similar to the ones shown in curve of S2. From the curve of S2, the corresponding sample is $Au/Co_3O_4$ composite. For preparation of S4, a certain amount of $AgNO_3$ had been added, and the final sample might contain Ag. However, the characteristic diffraction peaks of cubic Ag and Au at 2θ in the range from 20 to 70$^o$ all appear at the same positions, namely at 38, 44 and 64$^o$ corresponding to the identical planes of (111), (200) and (220), respectively. Hence, the diffraction peaks locating at 38, 44 and 64$^o$ belong to both cubic Ag and Au simultaneously. However, by distinguishing the (111) and (200) planes in curves of S2 and S4, their intensities in the curve of S4 are stronger than that in the curve of S2. The main reason is that S4 has not only the identical amount of Au like S2 but also a certain amount of Ag. So S4 is the composite of $Ag_xAu_y/Co_3O_4$. Additionally, all the diffraction peaks of the three samples broaden apparently, indicating their weak crystallinity and smaller sizes.

To further confirm the exact composition of the resultant sample, the XPS experiment was carried out by using S4. The result is exhibited in Fig.3. From the survey XPS spectrum, C1s peak locates 284.6 eV, and except C, Au, Ag, Co, and O elements, no peaks belonging to the other elements can be observed, which indicates that the corresponding sample is consisted of Au, Ag, Co and O elements. The tested contents of Au, Ag, Co and O elements are coincident to the values in $Ag_xAu_y/Co_3O_4$ with 2% Ag and 2% Au. The survey results of XPS experiment are further authenticated that the composite sample is $Ag_xAu_y/Co_3O_4$ composite.

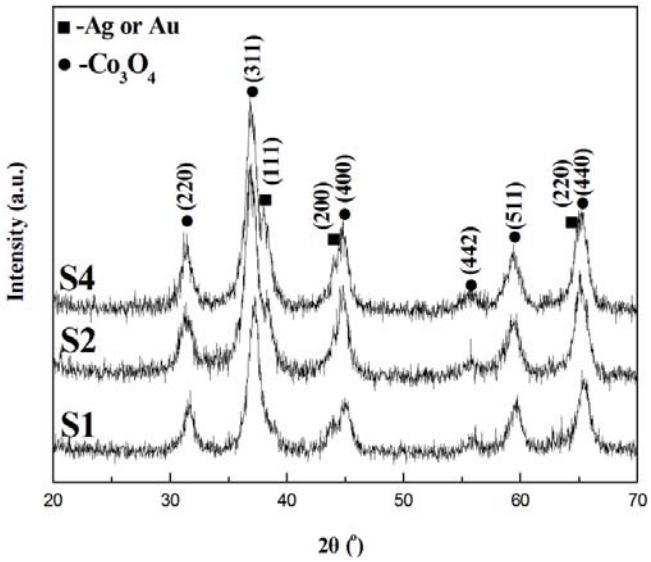


Fig. 2 – XRD patterns of S1, S2 and S4 samples.

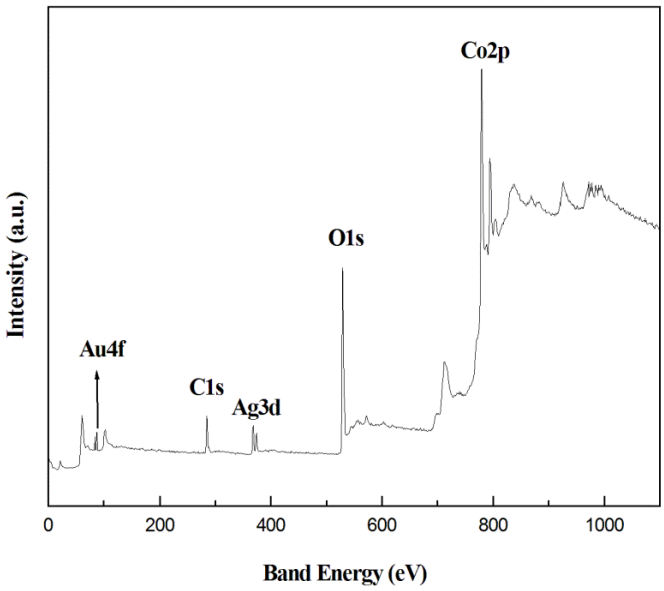


Fig. 3 – XPS curve of S4.

Fig. 4 shows the TEM images of S1 (a and b), S2 (c), S3(d), S4 (e and f) and S5(g), respectively. Fig.4a and b exhibit that $Co_3O_4$ has sheet-like morphology and these nanosheets have many caves. The formation of the caves is ascribed to rushing of gas molecules by calcining the precursor. Furthermore, the sizes of these nanosheets are not uniform. From Fig. 4c, S2 sample also presents sheet-like appearance. But by comparing carefully the images of S1 and S2, the S2 nanosheets are more disordered. But there are a few Au nanoparticles (represented in black dots) in S2 sample. The results indicated that addition of Au not only influences the morphology of $Co_3O_4$, but Au nanoparticles with a mean size of less than 10 nm have been dispersed on $Co_3O_4$ nanosheet. Fig.4e-g displays the morphologies of S3-S5. By comparison with the images of S2 and S3-S5, they have the similar nanosheet-like morphology. Furthermore, there are more black dots attributed to Ag and Au nanoparticles in Fig.4e-g (the magnified image of S4). From the magnified image shown in Fig.4e, not only both Ag and Au nanoparticles have the similar sizes but they have been dispersed finely on $Co_3O_4$ nanosheets. In the synthesis, the formation of $Co_3O_4$ nanosheets is ascribed to addition of sorbate salt. Without potassium sorbate, the resultant $Co_3O_4$ is nanoparticles (shown in Fig. 4f). Additionally, potassium sorbate also served as the reductant for Ag(I) and Au(III).

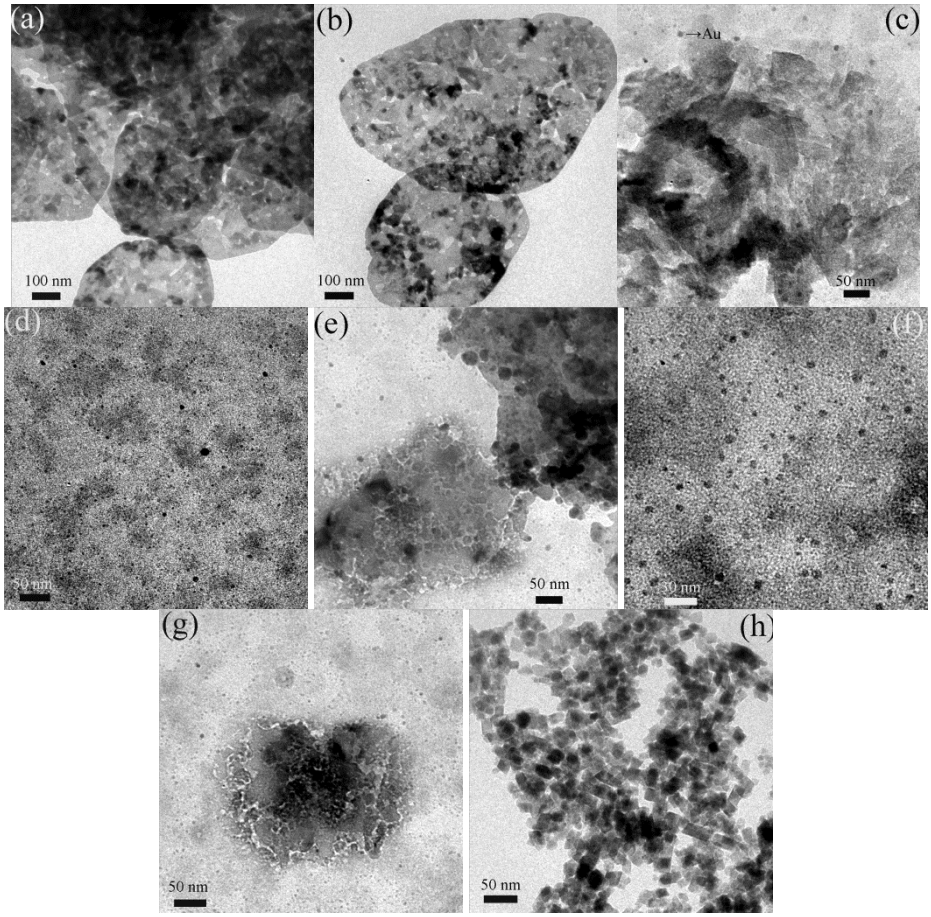


Fig. 4 – TEM images of S1 (a and b), S2 (c) , S3 (d), S4 (e and f), S5(g) and $Co_3O_4$ with addtion of potassium sorbate (h).

### 3. The electrocatalytic performances of the samples

Cyclic voltammorgrams of modified electrodes are tested frequently to reveal the electrocatalytic performances of samples. The electrocatalytic performances of as-synthesized $Co_3O_4$ and $Au/Co_3O_4$ and $Ag_xAu_y/Co_3O_4$ composites modified on a GCE for *p*-nitrophenol reduction in a basic solution were investigated, respectively. The results are displayed in Fig. 5. In the electrocatalytic experiments, the modified GCE served as the working electrode, a platinum electrode as the counter electrode and a Ag/AgC1 electrode as the reference electrode, respectively. According to Fig.5, a bare GCE has shown weak electrocatalytic activity for *p*-nitrophenol reduction, for its reduction peak current is rather lower (only 40 μA) at a comparatively higher peak potential at -1.15 V. As a GCE modified with from S1 to S5, respectively, the corresponding reduction peak potential and peak current are -1.05 V *vs.* 101 μA, -0.78 *vs.*119 μA, -0.71 *vs.*126 μA, -0.66 *vs.* 207 μA, and -0.66 V *vs.*230 μA, respectively. By comparison with a bare GCE, the modified GCEs with from S1 to S5, the peak current not only are 2.5, 3.0, 3.2, 5.2 and 5.7 times bigger than that with a bare GCE, but the corresponding potentials decreases with 0.10, 0.37, 0.44, 0.49 and 0.49 V, respectively. The results show that not only the peak currents increase but the corresponding peak potentials decrease (the peak potentials of both with S4 and S5 are same) as a GCE modified with the sample from S1 to S5 in turn, which indicates that the electrocatalytic activity of samples for *p*-nitrophenol reduction increases according to the order from S1 to S5 in turn. Especially the samples of S4 and S5 exhibit much higher electrocatalytic property. From the above results, as the $Co_3O_4$ loaded with Au nanoparticles, the $Au/Co_3O_4$ shows higher electrocataltyic activity than $Co_3O_4$, which suggests that doping of Au nanoparticles into $Co_3O_4$ is advantageous to transmission of the electrons. As the $Au/Co_3O_4$ nanosheets are doped with Ag nanoparticles, the elctrocatalytic performance rise in turn by increasing Ag content from 1 to 3%. The results demonstrate that Ag nanoparticles are more favorable the transmission of the electrons. Certainly, the experiments further proved that the

electrocatalytic activity might depress as Ag content in the $Ag_xAu_y/Co_3O_4$ composites increases. The main reason may be that Ag nanoparticles can aggregate as Ag content increases and the electrocatalytic centers may deduce. Similarly, increase of Au nanoparticles also can deduce the activity centers. Consequently, the suitable Ag and Au contents are needed be controlled at 2% or so.

The electrocatalytic experiments show that loading of Au and Ag nanoparticles on $Co_3O_4$ nanosheets can improve the electrocatalytic performances of $Co_3O_4$ nanosheets, for not only the peak currents increase but the peak potentials decrease obviously by using the GCE modified with S2 or S3 than the one with S1. From the curve 3 and 4 in Fig.5, the electrocatalytic performance of S3 is higher than S2, for the peak current increases slightly, but the peak potential decreases from -0.78 V to -0.71V, which suggests that Au and Ag may have a certain synergistic elecrocatalysis effect. It is well known that both Au and Ag have excellent electron transmission ability. The loading of both Au and Ag on $Co_3O_4$ nanosheets can enhance the electrocatalytic activity of the composites.

To explore the electrocatalytic mechanism, the effects of scanning rate on the catalytic activity were investigated using a GCE modified with S3, S4 and S5, respectively. The results show in Fig.6. From Fig.6, all the reduction peak currents increase by increasing scanning rate in the range from 0.02 to 0.10 $V \cdot s^{-1}$. It can be seen that the peak currents all increase linearly with the square root of scanning rate from 0.02–0.10 $V \cdot s^{-1}$ (all linearly dependent coefficients are more than 0.99), indicating *p*-nitrophenol reduction on the $Ag_xAu_y/Co_3O_4$/GCEs may be attributed to diffusion controlled reaction.[15]

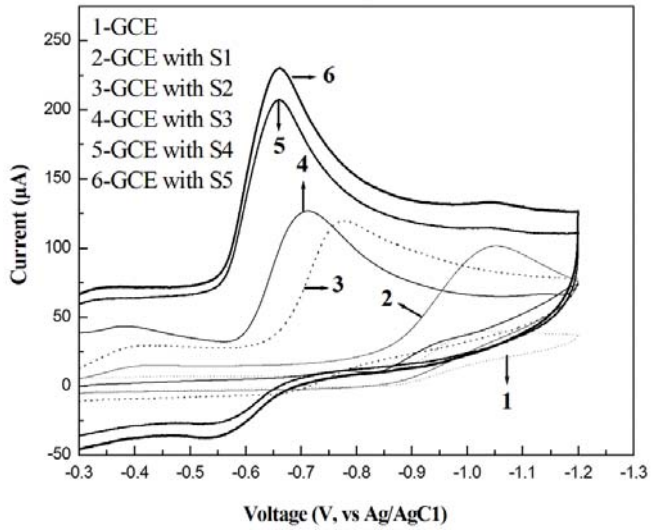


Fig. 5 – Cyclic voltammorgrams of a bare GCE and a GCE modified with $Co_3O_4$ (S1) and $Ag_xAu_y/Co_3O_4$ composites (S2-S5) in 1 $mol.L^{-1}$ NaOH +1.0 $mmol.L^{-1}$ *p*-nitrophenol (scanning rate 0.02 $V.s^{-1}$).

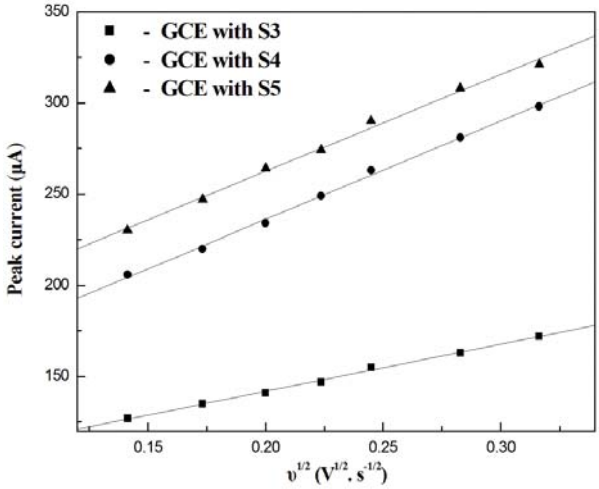


Fig. 6 – The plot of $I_{pc}$ *vs*. square root of scan rate with $Ag_xAu_y/Co_3O_4$ composites.

## CONCLUSIONS

Sheet-like $Co_3O_4$, Au/$Co_3O_4$ and $Ag_xAu_y$/$Co_3O_4$ composites could be fabricated by calcining their precursors synthesized via a combined precipitation-hydrothermal procedure at facile and easily controlled conditions. Ag and Au nanoparticles with the size less than 10 nm were dispersed evenly on the $Co_3O_4$ nanosheets with many caves. Electrocatalytic testing verified that doping of Au or Ag nanoparticles could enhance effectively the catalytic activity of $Co_3O_4$, and both Au and Ag nanoparticles might have the synergetic elctrocatalytic effect for the *p*-nitrophenol reduction. The $Ag_xAu_y$/$Co_3O_4$ composites with lower Au or Ag content (such as 2%) could exhibit higher electrocatalytic performance.

*Acknowledgements.* This study was supported by the Nature Science Fund of Anhui Province, China (Grant no. 1608085MB33 and 1808085ME109) and the University Nature Science Research Project of Anhui Province, China (Grant no. KJ2015A208), respectively.

## REFERENCES

1. G. Bai, H. Dai, J. Deng, Y. Liu, F. Wang, Z. Zhao, W. Qiu and C. T. Au, *Appl. Catal. A Gen.*, **2013**, *450,* 42-49.
2. W. J. Xue, Y. F. Wang, P. Li, A. T. Liu, Z. P. Hao and C. Y. Ma, *Catal. Commun.*, **2011**, *12*, 1265-1268.
3. N. Liu, P. Tao, C. Jing, W. Huang, X. Zhang and M. Wu, *J. Mater. Sci.*, **2018**, *53*, 15051-15063.
4. B. H. R. Suryanto, X. Lu and C. Zhao, *J. Mater. Chem. A*, **2013**, *1*, 12726-12731.
5. S. Park, S. Kim, H. Kheel and C. Lee, *Sensor Actuat. B Chem.,* **2015**, *58*, 26-47.
6. A. Mirzaei, S. Park, H. Kheel, G. J. Sun, T. Ko and S. Lee, *J. Nanosci. Nanotechnol.,* **2017**, *17*, 4087-4090.
7. K. C. Hsu and D. H. Chen, *Nanoscale. Res. Lett.*, **2014**, *9*, 484.
8. N. K. R. Bogireddy, U. Pal, L. Martinez Gomez and V. Agarwal, *RSC Adv.*, **2018**, *8*, 24819-24826.
9. L. Y. Chang, A. S. Barnard, L. C. Gontard and R. E. Dunin-Borkowski, *Nano Lett.,* **2010,** *10*, 3073-3076.
10. S. Cai, X. Liu, Q. Han, C. Qi, R. Yang and C. Wang, *Nano Res.*, **2018**, *11*, 3272-3281.
11. F. Yu and X. Zhang, *J. Energ. Chem.*, **2013**, *22*, 845-852.
12. S. Bao, N. Yan, X. Shi, R. Li and Q. Chen, *Appl. Catal. A Gen.*, **2014**, *487*, 189-194.
13. S. Muhammad, M. Majid, M. Nida, S. Mohsin, A. Nadia and H. Muhammad, *Chinese J. Chem. Eng.*, **2018**, *26*, 1264-1269.
14. S. Miao and Y. Deng, *Appl. Catal. B Environ.*, **2001**, *31*, L1-L4.
15. S. G. Wu, L. Z. Zheng, L. Rui and X. Q. Lin, *Electroanalysis*, **2001**, *13,* 967-970.